References

[1]"Assessment of Experimental Uncertainty with Application to Wind Tunnel Testing," AIAA Standard S-071A-1999, Revision A of the Standard, AIAA, Reston, VA, 1999, pp. 11–17.

[2]Coleman, H. W., and Steele, W. G., *Experimentation and Uncertainty Analysis for Engineers*, 2nd ed., Wiley, New York, 1999, pp. 83–88, Eqs. (4.2–4.8).

[3]Meyn, L. A., "An Uncertainty Propagation Methodology That Simplifies Uncertainty Analyses," AIAA Paper 2000-0149, Jan. 2000; Eqs. (4–12).

[4]Forsythe, G. E., Malcolm, M. A., and Moler, C. B., *Computer Methods for Mathematical Computations*, Prentice–Hall, Englewood Cliffs, NJ, 1977, pp. 13, 14, 41.

[5]Press, W. H., Teukolsky, S. A., Vetterling, W. T., and Flannery, B. P., *Numerical Recipes in FORTRAN 77*, 2nd ed., Cambridge Univ. Press, Cambridge, England, U.K., 1996, pp. 180–182.

S. K. Aggarwal
Associate Editor

Rapid Scanning of Overheat Ratios Using a Constant Voltage Anemometer

Joseph D. Norris* and Ndaona Chokani†
North Carolina State University, Raleigh, North Carolina 27695

THE requirements of large bandwidth and high spatial resolution have resulted in thermal hot-wire anemometry being the most widely used tool for the measurement of freestream and boundary-layer/shear-layer fluctuations in high-speed flows. When there is also a need to derive the fluctuations in terms of gas dynamic parameters, this measurement task is more challenging because the hot wire has a mixed mode response to both mass flux and total temperature and the hot wire must be operated at multiple overheats. Furthermore, as most high-speed facilities have relatively short run times, it is highly desirable that these multiple overheats are accomplished within a single run to ensure accuracy in the measured data. The two common modes of operating the hot-wire are the constant-current anemometer (CCA) and the constant-temperature anemometer (CTA). More recently the constant voltage anemometer (CVA) has been introduced by Sarma.[1] In comparison to the CCA and CTA, the CVA's advantages include larger bandwidths, lower electronic noise, and higher sensitivity. The CVA-operated hot wire has been used to characterize the evolution of the transitional hypersonic boundary-layer disturbances by Lachowicz et al.[2] and Doggett et al.[3] The fluctuations in a turbulent supersonic boundary layer have also been documented using the CVA by Comte-Bellot and Sarma[4] and Weiss et al.[5]

Walker et al.[6] demonstrated the rapid scanning of multiple overheats in a CTA to resolve the mass flux and total temperature fluctuations in a supersonic flow. The overheat was stepped through eight operating temperatures at a rate of 10 ms/temperature; the temperature was increased from step to step. More recently, Weiss et al.[7] described the application of a CTA with automatic rapid scanning to measure at six overheats over a test time of 120 ms; the scanning was demonstrated for decreasing values of the overheats. The rapid scanning of multiple overheats using a CTA operation is however problematic because of the coupled frequency response and overheat behavior in the CTA. The frequency response of the CTA can be inferred from the following equation[8]:

$$M_{\mathrm{CTA}} = M_{\mathrm{wire}}/(1 + 2a_w R_w G) \tag{1}$$

where a_w and R_w are the overheat and resistance of the hot wire, respectively, G is the transconductance of the CTA, and M_{CTA} and M_{wire} are the time constants of the CTA and the hot wire, respectively. The CTA bridge can be balanced for an optimum bandwidth for only one overheat; thus, when the bridge is adjusted at the lowest overheat, the bridge becomes unstable at higher overheats. On the other hand, when the bridge is balanced at the highest overheat, its bandwidth decreases with decreasing overheat, Eq. (1).[7] Thus with the rapid scanning of multiple overheats in a CTA, the measurements are either obtained over a small range of overheats or with different bandwidths at each overheat.

The CVA is a second-order system, whose expressions for the hardware time constant T_c, natural frequency ω_n, damping ratio ζ, and bandwidth BW are given in Sarma et al.[9]:

$$T_c = \frac{C R_a R_b}{R_2}, \qquad \omega_n = \sqrt{\frac{R_w}{R_2}\frac{2\pi f_t}{T_c}\left(1 + \frac{R_2}{R_d}\right)}$$

$$\zeta = \frac{1}{2}\left[\left(\frac{1}{T_c} + 2\pi f_t \frac{R_w}{R_d}\right) \Bigg/ \sqrt{\frac{R_w}{R_2}\frac{2\pi f_t}{T_c}\left(1 + \frac{R_2}{R_d}\right)}\right]$$

$$BW = \omega_n \sqrt{(1 - 2\zeta^2) + \sqrt{4\zeta^4 - 4\zeta^2 + 2}} \tag{2}$$

where f_t is the gain bandwidth of the operational amplifier in the CVA circuit (Fig. 1) and

$$1/R_2 = 1/(R_a + R_b) + 1/R_d$$

Sarma[10] has theoretically shown, and Kegerise and Spina[11] have experimentally established, that the bandwidth of the CVA does not change with overheat. This constant bandwidth feature of the CVA coupled with its demonstrated attributes of large bandwidth, low electronic noise, and high sensitivity make it extremely attractive for obtaining calibrated measurements in short-run-time, high-speed facilities. In all of the aforementioned CVA applications,[2–5,9] continuous running high-speed facilities were used. In the present Note we demonstrate the application of the CVA in a short-run-time supersonic wind-tunnel facility.

The associated circuit of the Tao Systems® Model VC-01 CVA used in the present work is shown in Fig. 1. The wire voltage V_w is given in Ref. 10 as

$$V_w = (R_F/R_1)V_1 \tag{3}$$

In the present work a programmable Wavetek® arbitrary waveform generator is used to vary V_1 (and thus V_w and a_w) in six stepped increments with a duration of 20-ms/wire voltage (Fig. 2). A Nicolet®

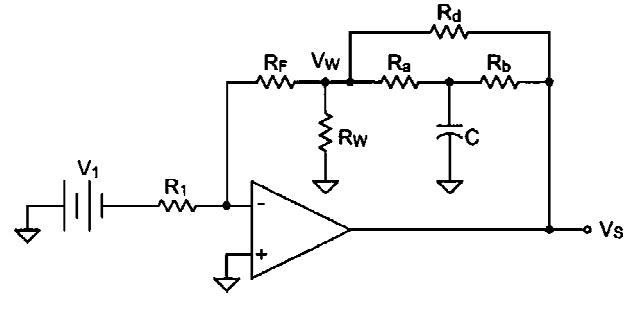

Fig. 1 Compensated CVA circuit (from Ref. 10).

Received 14 October 2002; revision received 10 February 2003; accepted for publication 17 February 2003.

*Research Assistant, Department of Mechanical and Aerospace Engineering; currently Aerospace Engineer, Sverdrup Corporation, Silver Spring, MD 20903. Student Member AIAA.

†Professor, Department of Mechanical and Aerospace Engineering. Associate Fellow AIAA.

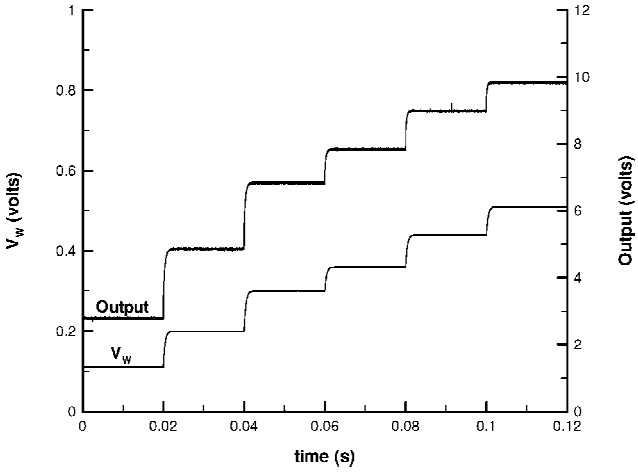

Fig. 2 Hot-wire voltage and anemometer dc output with automated stepping.

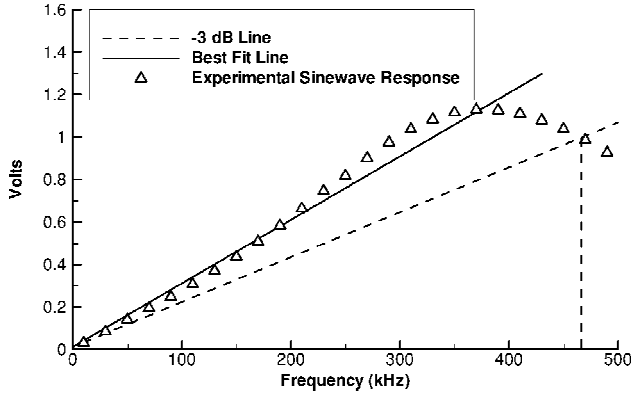

Fig. 3 Sine-wave response of Tao Systems CVA Model VC-01.

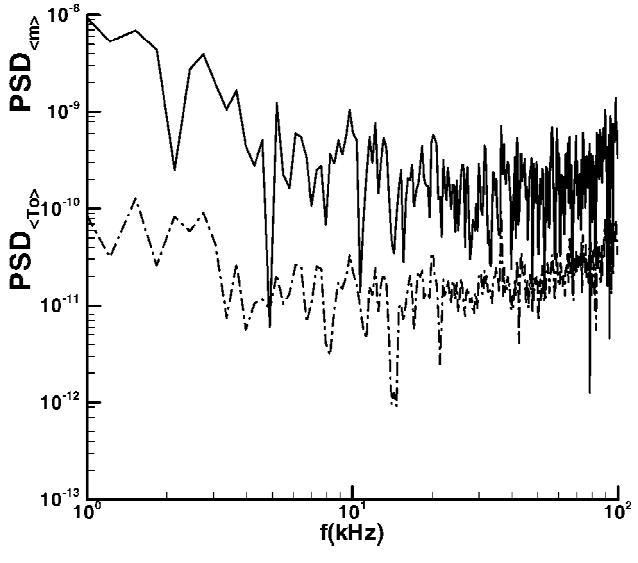

Fig. 4 Power spectral densities of mass flux (——) and total temperature (– – –).

digital oscilloscope is used to sample the anemometer output voltage V_s at 2.5 MHz. The bandwidth of the CVA was verified by the sine-wave signal injection test.[10] The sine-wave response is shown in Fig. 3; the 3-dB line intersects the sine-wave response at 470 kHz. As the CVA bandwidth does not change with overheat, this measured bandwidth is the actual bandwidth of the CVA.

The experiments were conducted in the shock wind tunnel (SWK) at Universität Stuttgart; the facility is described in Knauss et al.[12] The principle of the SWK operation is that of a shock tube with Laval nozzle. The test section of SWK is 1.2×0.8 m^2, the test section Mach number is 2.54, and the flow duration is approximately 120 ms. The results of the tests conducted at a unit Reynolds number of 10×10^6/m are presented here. Two runs were conducted with six stepped voltages in each run; the ranges of overheat in each run were 0.05–0.56 and 0.56–1.06, respectively.

The hot wire has a mixed mode response to mass flux m and total temperature T_0 (Ref. 13):

$$e'/E = S_m(m'/\bar{m}) + S_{T_0}(T_0'/\overline{T_0}) \tag{4}$$

where e', E are the fluctuating and mean CVA output voltages, respectively; and S_m and S_{T_0} are the relative sensitivities. Squaring and averaging Eq. (4) and then rewriting yields

$$\overline{e'^2}/S_{T_0}^2 E^2 = \left(S_m^2/S_{T_0}^2\right)(\overline{m'^2}/\bar{m}^2) + 2\left(S_m/S_{T_0}\right)(\overline{m'T_0'}/\bar{m}\bar{T}_0) + \overline{T_0'^2}/\bar{T}_0^2 \tag{5}$$

The ratio $S_m/|S_{T_0}|$ is simply $a_w/2$ and $S_{T_0} \cong -1/(1+2a_w)$ (Ref. 14). For a hot wire operated at multiple overheats, the Fourier transform analysis of Eq. (5) then yields the power spectral densities of mass flux and total temperature. The measured power spectra are shown in Fig. 4. These spectra show the characteristics of a turbulent nozzle flow that radiates sound waves into the freestream.[15] It is also seen that the total temperature fluctuations are two orders of magnitude smaller than the mass flux fluctuations. These measurements confirm that SWK has low-level freestream disturbances. This CVA demonstration is an advancement over previous works that employed CTA, as the latter approach has a different bandwidth at each overheat, whereas the CVA has a fixed bandwidth.

Acknowledgments

This work is supported by the U.S. Air Force Office of Scientific Research under Grants F49620-01-1-0105 and F49620-01-1-0244. The Technical Monitor is John D. Schmisseur. The authors are sincerely grateful to Garimella R. Sarma of Tao Systems for many discussions concerning the use of the constant-voltage anemometer. The authors also gratefully acknowledge the assistance of Helmut Knauss, Uwe Gaisbauer, Karl Heinz Laicher, and Julien Weiss (Universität Stuttgart), Geneviève Comte-Bellot (Ecole Centrale de Lyon), and Alexander D. Kosinov (Russian Academy of Sciences—Siberian Branch) during the conduct of the experiments.

References

[1]Sarma, G. R., "Flow Measuring Apparatus," U.S. Patent 5074147, Dec. 1991.

[2]Lachowicz, J. T., Chokani, N., and Wilkinson, S. P., "Boundary-Layer Stability Measurements in a Hypersonic Quiet Tunnel," *AIAA Journal*, Vol. 34, No. 12, 1996, pp. 2496–2500.

[3]Doggett, G. P., Chokani, N., and Wilkinson, S. P., "Effects of Angle of Attack on Hypersonic Boundary Layer Stability in a Quiet Wind Tunnel," *AIAA Journal*, Vol. 35, No. 3, 1997, pp. 464–470.

[4]Comte-Bellot, G., and Sarma, G. R., "Constant Voltage Anemometer Practice in Supersonic Flows," *AIAA Journal*, Vol. 39, No. 2, 2001, pp. 261–270.

[5]Weiss, J., Knauss, H., Wagner, S., Chokani, N., Comte-Bellot, G., and Kosinov, A. D., "Comparative Measurements in $M_\infty = 2.54$ Flow Using Constant-Temperature and Constant-Voltage Anemometers," AIAA Paper 2003-1277, Jan. 2003.

[6]Walker, D. A., Ng, W. F., and Walker, M. D., "Experimental Comparison of Two Hot-Wire Techniques in Supersonic Flow," *AIAA Journal*, Vol. 27, No. 8, 1989, pp. 1074–1080.

[7]Weiss, J., Knauss, H., Wagner, S., and Kosinov, A. D., "Constant Temperature Hot-Wire Measurements in a Short Duration Supersonic Wind Tunnel," *Aeronautical Journal*, Vol. 105, Aug. 2001, pp. 435–441.

[8]Owen, F. K., Horstman, C. C., and Kussoy, M. I., "Mean and Fluctuating Flow Measurements of a Fully-Developed, Non-Adiabatic, Hypersonic Boundary Layer," *Journal of Fluid Mechanics*, Vol. 70, Pt. 2, 1975, pp. 393–413.

[9]Sarma, G. R., Comte-Bellot, G., and Faure, T. M., "Software Corrected Hot Wire Thermal Lag for the Constant Voltage Anemometer Featuring a Constant Bandwidth at the Selected Compensation Setting," *Review of Scientific Instruments*, Vol. 69, No. 9, 1998, pp. 3223–3231.

[10]Sarma, G. R., "Transfer Function Analysis of the Constant Voltage Anemometer," *Review of Scientific Instruments*, Vol. 69, No. 6, 1998, pp. 2385–2391.

[11]Kegerise, M. A., and Spina, E. F., "A Comparative Study of Constant-Voltage and Constant-Temperature Hot-Wire Anemometers: Part II—The Dynamic Response," *Experiments in Fluids*, Vol. 29, No. 2, 2000, pp. 165–177.

[12]Knauss, H., Riedel, R., and Wagner, S., "The Shock Wind Tunnel of Stuttgart University: A Facility for Testing Hypersonic Vehicles," AIAA Paper 99-4959, Nov. 1999.

[13]Morkovin, M. V., "Fluctuations and Hot-Wire Anemometry in Compressible Flows," AGARDograph 24, Nov. 1956.

[14]Comte-Bellot, G., "Hot-Wire Anemometry," *Handbook of Fluid Dynamics*, edited by R. W. Johnson, CRC Press, Boca Raton, FL, 1998, Chap. 34.

[15]Chen, F.-J., Malik, M. R., and Beckwith, I. E., "Görtler Instability and Supersonic Quiet Nozzle Design," *AIAA Journal*, Vol. 30, No. 8, 1992, pp. 2093, 2094.

R. P. Lucht
Associate Editor

Numerical Instability of Classical Free-Interface Component Mode Synthesis Techniques

Ronnie Bladh,* Christophe Pierre,† and Matthew P. Castanier‡
University of Michigan, Ann Arbor, Michigan 48109-2125

Nomenclature

$\boldsymbol{f}_\Gamma$	=	interface force vector
$\boldsymbol{G}$	=	flexibility matrix
$\boldsymbol{G}^r$, $\boldsymbol{H}^r$	=	residual flexibility matrix, residual inertia matrix
$\boldsymbol{K}$, $\boldsymbol{M}$	=	stiffness matrix, mass matrix
$\boldsymbol{p}$	=	generalized (modal) coordinates
$\boldsymbol{x}$	=	physical (finite element) coordinates
$\boldsymbol{\kappa}$, $\boldsymbol{\mu}$	=	condensed stiffness matrix, condensed mass matrix
$\boldsymbol{\Lambda}$	=	diagonal matrix of eigenvalues of the kept component normal modes
$\boldsymbol{\Phi}$	=	set of kept component normal modes
$\boldsymbol{\Psi}$	=	set of all residual attachment modes
$\boldsymbol{\Psi}_\Gamma^{r,1}$, $\boldsymbol{\Psi}_\Gamma^{r,2}$	=	first-order and second-order residual deflections of the interface degrees of freedom (DOF)
ω	=	frequency

Subscripts

k	=	coordinates of the kept component normal modes
r	=	coordinates of the residual flexibility modes
Γ	=	finite element DOF of the component interface
Δ	=	finite element DOF of the component interior

Superscripts

α, β	=	the corresponding component

Received 21 June 2002; revision received 25 March 2003; accepted for publication 3 April 2003.

*Visiting Research Investigator, Department of Mechanical Engineering; currently Development Engineer, ALSTOM Power, 612 82 Finspang, Sweden.

†Professor, Department of Mechanical Engineering; pierre@umich.edu. Senior Member AIAA.

‡Associate Research Scientist, Department of Mechanical Engineering, 2279 G. G. Brown Building; mpc@umich.edu. Senior Member AIAA.

Introduction

FINITE element based component mode synthesis[1] (CMS) techniques are popular tools used in structural dynamics applications. In CMS, the original structure is subdivided into smaller substructures, or components, for which normal modes are computed independently and more inexpensively. The assembled system is then represented by a truncated set of component modes through necessary compatibility constraints applied in a systematic fashion. This process yields reduced-order models based on parent finite element models of arbitrary complexity. CMS techniques are usually characterized by the manner in which the component normal modes are computed: 1) with fixed interfaces or 2) with free interfaces.

In general, the classical CMS methods perform very well, yielding accurate reduced-order models. For free-interface CMS,[2] the successful methods are those that account for the effects of neglected (residual) modes, such as the methods formulated by Rubin[3] and by Craig and Chang.[4] However, it is shown in this study that free-interface CMS methods incorporating residual effects do have built-in numerical instability. This is due to matrix ill-conditioning that occurs when there are only very small residual contributions, for example, for large numbers of retained component modes. This numerical instability appears abruptly and can have a devastating effect on the accuracy of these methods because any likeness to the behavior of the parent finite element model vanishes. Moreover, there are no means of determining the onset of these problems a priori. As far as the authors are aware, this limitation of the classical free-interface CMS methods has not been documented in the open literature.

In all fairness, note that the reported numerical instability is unlikely to be of concern for most engineering applications because typically only a small fraction of the total number of component modes is retained. Furthermore, this instability does not exist for fixed-interface CMS methods, which are not considered here. However, for certain special applications of free-interface CMS methods, it may be critically important to be aware of this numerical instability. One such special case was encountered by the authors in their line of research on the modeling of mistuned bladed disks using secondary modal analysis reduction techniques.[5] This type of modeling technique involves a two-step approach: First, CMS is used to isolate blade properties for direct perturbations (blade mistuning). Second, a modal analysis is performed on the CMS model to generate a small reduced-order model based on the global modes in a frequency range of interest. In this case, the primary purpose of using CMS is to cast the original finite element model in a form that is better suited for input of blade mistuning, rather than to achieve model reduction. Therefore, for simpler academic models used in parameter studies, where high model accuracy is desired, the number of retained component modes may well surpass the unknown stability limit.

In this work, two classical free-interface CMS methods[3,4] are briefly reviewed, and the sources of numerical instability are highlighted. In addition, a modest modification to the classical free-interface CMS formulation by Craig and Chang[4] is presented, which alleviates the numerical instability suffered by the original method. To support the discussion, the numerical instability is demonstrated with a simple three-dimensional, two-component finite element model.

Sources of Numerical Instability in Classical Free-Interface CMS

Craig–Chang Method[4]

The Craig–Chang (C^2) method[4] uses as a component modal basis a truncated set of kept component normal modes of vibration, where all of the degrees of freedom (DOF) on interfaces with adjacent components are free. A complete set of residual attachment modes are then used to supplement the normal modes. The residual attachment modes represent purely computational shapes induced in the residual structure (i.e., after removing the flexibility represented by the kept normal modes) by successively applied unit loads on each interface DOF, with all other interface DOF free and unloaded. If the